Optics Communications 285 (2012) 5549–5553

Contents lists available at SciVerse ScienceDirect

Optics Communications

journal homepage: www.elsevier.com/locate/optcom

Compact generation of polarization-frequency hyperentangled photon pairs by using quasi-phase-matched lithium niobate

Jin Shi [a,b], Su-Jun Yun [a], Yan-Fei Bai [a], Ping Xu [a,*], Shi-Ning Zhu [a]

[a] National Laboratory of Solid State Microstructures and School of Physics, Nanjing University, Nanjing 210093, China
[b] School of Physics and Electronic Electrical Engineering, Huaiyin Normal University, Huaian 223300, China

ARTICLE INFO

Article history:
Received 4 March 2012
Received in revised form
6 July 2012
Accepted 30 July 2012
Available online 6 September 2012

Keywords:
Hyperentangled photon-pair
Lithium niobate
Quasi-phase-matching

ABSTRACT

We propose a compact generation of polarization-frequency hyperentangled photon-pair source emitting at a telecom wavelength by engineering a multi-stripe lithium niobate bulk crystal. Each stripe is designed to be poled following a dual-periodic structure and serves for a nondegenerate cross-polarization-entanglement generation. The frequency of photon pair from each stripe differs, thus resulting in a high-dimensional frequency-entanglement. The degree of entanglement and temperature-detuning character of the hyperentangled state are analyzed. Furthermore, another feasible experiment realization of such a photon source is proposed based on guided-wave optics which improves the performance with high brightness, miniaturization and stabilization. Such high-dimensional frequency and cross-polarization hyperentangled photon pairs will have potential applications in quantum communication networks.

1. Introduction

Photon pairs generated from spontaneous parametric down conversion (SPDC) have a variety of accessible degrees of freedom (DOFs) like polarization, time-bin, frequency, orbital angular momentum or spatial mode. Each degree of freedom can be exploited for the entanglement production. Such an entangled state plays a critical role in quantum information processing [1–3]. How to effectively expand the number of entangled qubits is a serious challenge. One of the schemes is to engineer a simultaneous entanglement over multiple DOFs, referred to as hyperentanglement [4]. It can enlarge the Hilbert space, thereby improve the performance of many tasks in quantum information science such as enhancing the channel capacity in super dense coding [5], quantum key distribution [6] and assisting the complete Bell-state discrimination [7–9]. The hyperentanglement has been experimentally realized from nonlinear crystals and external linear optical elements are usually adopted [10–12]. How to simplify the experimental realization and also how to obtain hyperentangled photon pairs with higher brightness have become crucial problems in quantum information science.

Quasi-phase-matching (QPM) material opens a new way to engineer high-flux entangled photon pairs [13] and also enable new types of two-photon state with unique spatial entanglement [14,15], or frequency spectrum [16–18]. In this paper, we propose a compact polarization-frequency hyperentangled photon source from a multi-stripe dual-periodic poled lithium niobate (DPPLN) bulk crystal. We design each stripe to provide concurrent two type-II QPM SPDC processes for nondegenerate photon-pair generation, yielding a post-selection free polarization-entanglement generation. The photon pairs from each stripe have different frequency, and result in a comb-spectrum locating at the fiber communication wavelength. Besides, we also discuss the feasible realization of this hyperentangled photon source based on guided-wave optics. The compact hyperentangled photon source will have potential applications in quantum information science such as the wavelength-division multiplexing (WDM) for quantum communication networks.

2. Structure design and theoretical analysis

The QPM material has been applied to generate polarization-entangled state [19–24]. As one of the QPM materials, dual-periodic superlattice [24–26] can provide two reciprocal vectors hence two QPM SPDC processes will take place simultaneously. Here we design the DPPLN crystal for cross-polarization-entangled photon-pair generation at telecom wavelength. If the superlattice contains N-stripe and the frequency of photon pair from each stripe differs, then the N-dimensional frequency-entangled and nondegenerate cross-polarization-entangled state expressed as Eq. (1) can be generated. It is worth noting that the N-dimensional frequency-entangled state can only be obtained after we collect photons from each stripe into the same spatial

* Corresponding author.
E-mail address: pingxu520@nju.edu.cn (P. Xu).

0030-4018/$ - see front matter © 2012 Elsevier B.V. All rights reserved.
http://dx.doi.org/10.1016/j.optcom.2012.07.118

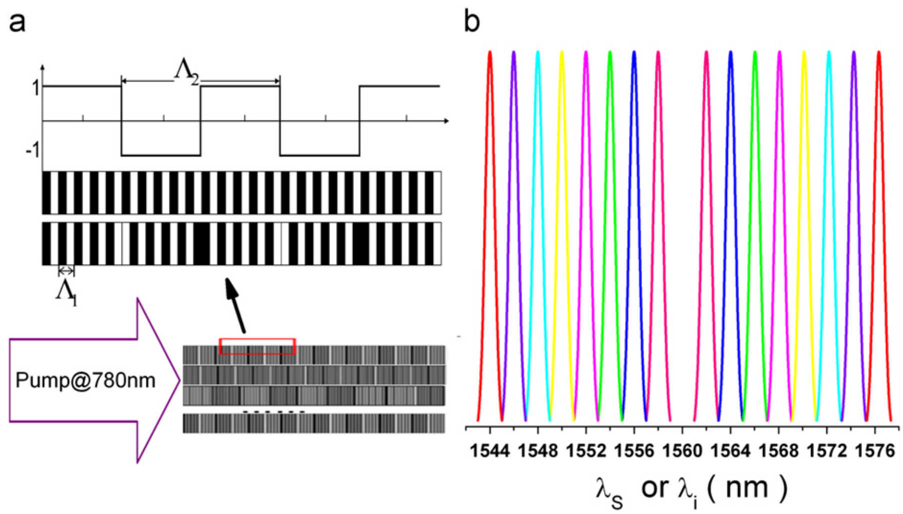

Fig. 1. Schematic description of N-dimensional frequency and cross-polarized hyperentanglement photon-pair generation by type-II SPDC in an N-stripe DPPLN bulk crystal.

mode, thus the path information is erased

$$\sum_{n=1}^{N} |\omega_{s_n}\omega_{i_n}\rangle (C_{oe}^{(n)}|HV\rangle + C_{eo}^{(n)}|VH\rangle). \tag{1}$$

Fig. 1 is the schematic description of N-dimensional hyper-entangled photon-pairs generation. The inset in the top corner of Fig. 1(a) depicts the structure design of a twice-periodic QPM materials [24–26]. Fig. 1(b) is the designed comb spectrum when the multi-stripe crystal is pumped by 780 nm. We label two poling periods as Λ_1 and Λ_2 ($\Lambda_1 < \Lambda_2$). Such a DPPLN is designed to ensure concurrent two type-II QPM SPDC processes for non-degenerate photon-pair generation under the conditions of energy conservation and momentum conservation

$$\omega_p = \omega_s + \omega_i, \tag{2}$$

$$\vec{k}_p = \vec{k}_s + \vec{k}_i + \vec{G}_{l,m}, \tag{3}$$

where p, s and i represent the pump photon, the down-converted signal and idler photons. The reciprocal vectors of dual-periodic superlattice take the form of [27]

$$G_{l,m} = G_l + G_m = \frac{2\pi l}{\Lambda_1} + \frac{2\pi m}{\Lambda_2}, \tag{4}$$

where nonzero integers l and m indicate the orders of reciprocal vectors. As Λ_1 and Λ_2 are independent of each other, the structure can provide two independent reciprocal vectors to quasi-phase-match two different SPDC processes simultaneously. Fourier coefficients are

$$f_{l,m} = \frac{2\sin(D_1 l\pi)}{l\pi}\frac{2\sin(D_2 m\pi)}{m\pi}. \tag{5}$$

We choose the duty cycles $D_1 = D_2 = 0.5$, and $l = 1$, $m = \pm 1$. We choose $G_{1,1}$ to work for the extraordinary (vertical polarization) signal and ordinary (horizontal polarization) idler photon-pair generation while $G_{1,-1}$ to work for the ordinary signal and extraordinary idler photon-pair generation both from the ordinary pump photon. Besides, to avoid the small domains, Λ_2 and Λ_1 should be commensurable so that the Fourier coefficients will not deviate too much from the theoretical design. Each stripe is designed to emit such a nondegenerate polarization-entangled state but the frequency of photon pair from each stripe is different thus the poling periods of Λ_1 and Λ_2 are different. Using multi-mode description of SPDC, we obtain the interaction Hamiltonian inside such a multi-stripe DPPLN crystal [27–30]

$$\hat{H}_I = \sum_{n=1}^{N} \varepsilon_0 \int_V d^3 r (\chi_A^{(2)} \hat{E}_p^{(+)} \hat{E}_{s_n,e}^{(-)} \hat{E}_{i_n,o}^{(-)} + \chi_B^{(2)} \hat{E}_p^{(+)} \hat{E}_{s_n,o}^{(-)} \hat{E}_{i_n,e}^{(-)}) + H.c, \tag{6}$$

where V denotes the interaction volume. The pump field is assumed to be plane wave and nondepleted classical field. $\hat{E}_p^{(+)}(\vec{r},t) = E_p e^{i(\vec{k}_p \cdot \vec{r} - \omega_p t)}$, while the signal and idler fields are considered to be nonclassical and represented by quantum operators

$$\hat{E}_j^{(-)} = \int d\omega_j \sqrt{\frac{\hbar\omega_j}{4\pi c\varepsilon_0 n_j(\omega_j) S}} \hat{a}_j^{+}(\omega_j) e^{i(\vec{k}_j \cdot \vec{r} - \omega_j t)}, \tag{7}$$

where S denotes the transverse area of pump beam, $j = s,i$. n_j represents refractive index. We consider the bandwidth of the down-converted beams and introduce a detuning variable v, defined as [28]

$$\omega_p = \omega_s + \omega_i = (\Omega_s - v) + (\Omega_i + v), \tag{8}$$

where $|v| \ll \Omega_s$, Ω_i. Using the first-order perturbation approximation in the interaction picture, we can obtain the output entangled state as

$$|\Phi\rangle = \sum_{n=1}^{N} \left(\int dv C_{eo}^{(n)} \Psi(\Delta k_{A_n} L) \hat{a}_{s_n e}^{+} \hat{a}_{i_n o}^{+} |0\rangle + \int dv C_{oe}^{(n)} \Psi(\Delta k_{B_n} L) \hat{a}_{s_n o}^{+} \hat{a}_{i_n e}^{+} |0\rangle \right), \tag{9}$$

in which L denotes the crystal length, $\Delta k_{A_n} = \vec{k}_p - \vec{k}_{s_n e} - \vec{k}_{i_n o} - \vec{G}_{1,1}$ and $\Delta k_{B_n} = \vec{k}_p - \vec{k}_{s_n o} - \vec{k}_{i_n e} - \vec{G}_{1,-1}$. $\Psi(\Delta kL)$ determines the bandwidth of two-photon state and takes the following form [27,28]:

$$\Psi(\Delta kL) = e^{-i\Delta kL/2} \mathrm{sinc}\frac{\Delta kL}{2}. \tag{10}$$

The coefficients $C_{eo}^{(n)}$ and $C_{oe}^{(n)}$ can be expressed as follows:

$$C_{eo}^{(n)} = d_{24} L f_{1,1} \frac{iE_p}{2c} \sqrt{\frac{\Omega_{s_n e}\Omega_{i_n o}}{n_{s_n e} n_{i_n o}}}, \tag{11}$$

$$C_{oe}^{(n)} = d_{24} L f_{1,-1} \frac{iE_p}{2c} \sqrt{\frac{\Omega_{s_n o}\Omega_{i_n e}}{n_{s_n o} n_{i_n e}}}. \tag{12}$$

We quantify the output state to be maximally entangled or not by defining a parameter γ as [24]

$$\gamma = \frac{\min(C_{eo}^{(n)}, C_{oe}^{(n)})}{\max(C_{eo}^{(n)}, C_{oe}^{(n)})}, \tag{13}$$

where $0 \le \gamma \le 1$, $\gamma = 1$ indicates a maximally entangled state and $\gamma = 0$ indicates an orthogonal state.

3. Results and discussions

With different wavelengths of incident pump light, the relationships between the parameter γ and the wavelength of the signal photon or idler photon are shown in Fig. 2. We can see γ becomes larger and tends to 1 as the signal and idler photons are degenerate.

Fig. 3 shows the detuning of signal or idler wavelength as a function of the grating period for two different SPDC processes converting an ordinary pump photon into $|HV\rangle$ and $|VH\rangle$ photon pair, simultaneously. It can be seen that for each pair of frequency, usually two different reciprocal vectors are required to satisfy both SPDC processes. The degenerate cross-polarization-entangled photon pair is generated at the point of intersection of two curves. For further calculations, we design a three-stripe DPPLN crystal which covers the wavelengths of 1552 nm/1568 nm, 1554 nm/1566 nm and 1556 nm/1564 nm when the pump is 780 nm. The wavelength separation is larger than the bandwidth of down-converted photons which is calculated to be roughly 98 GHz ($\triangle\lambda = 0.787$ nm at $\lambda = 1552$ nm). The working temperature is designed to be 160 °C. For the three-dimensional frequency and cross-polarization hyperentangled state generation, the involved reciprocal vectors for $|HV\rangle$ are 0.656481 μm^{-1}, 0.656676 μm^{-1}, 0.656872 μm^{-1} and the other set reciprocal vectors for $|VH\rangle$ are 0.657651 μm^{-1}, 0.657456 μm^{-1}, 0.657261 μm^{-1}. For the designed three pairs of reciprocal vectors, the wavelength of signal or idler photon varies as a function of the working temperature which is illustrated in Fig. 4. When the working temperature reaches 160 °C, two sets of tuning curves have six intersection points which imply that a three-dimensional frequency and cross-polarization hyper-entangled state is generated. When the temperature deviates from the designed working temperature, the $|HV\rangle$ and $|VH\rangle$ will associate with different frequency pairs, thus the frequency-polarization will not be hyperentangled. The hyperentanglement can be generalized into N-dimensional frequency entangled state if we design an N-stripe structure.

The photon-pairs generation rate can be calculated from $R = \sum_{n=1}^{N} \int_{-\infty}^{+\infty} d\omega_{s_n} \langle \Phi | \hat{a}^+(\omega_{s_n}) \hat{a}(\omega_{s_n}) | \Phi \rangle$. So we can get the generation rate of photon pairs [30]

$$R = \frac{L^2 E_p^2 d_{24}^2}{4c^2} \sum_n \int_{-\infty}^{+\infty} d\omega_{s_n} \left[\frac{f_{1,1}^2 \Omega_{s_n e} \Omega_{i_n o}}{n_{s_n e} n_{i_n o}} \Psi(\Delta k_{A_n} L)^2 + \frac{f_{1,-1}^2 \Omega_{s_n o} \Omega_{i_n e}}{n_{s_n o} n_{i_n e}} \Psi(\Delta k_{B_n} L)^2 \right]. \tag{14}$$

By substituting $|E_p|^2 = 2P/\varepsilon_0 n_p c S$, we can obtain

$$R = \frac{16 P L d_{24}^2}{\pi^3 \varepsilon_0 n_p c^3 S} \sum_n \left(\frac{\Omega_{s_n e} \Omega_{i_n o}}{D_{A_n} n_{s_n e} n_{i_n o}} + \frac{\Omega_{s_n o} \Omega_{i_n e}}{D_{B_n} n_{s_n o} n_{i_n e}} \right), \tag{15}$$

where P denotes the pump power. D_n is the group dispersion of the nth frequency pair. For example, we set $P = 1.0$ mW, $S = 3$ mm^2, L=20 mm, $d_{24} = 4.6$ pm/V [43]. Suppose the stripe spacing is small, then the generation rate of the nondegenerate source is found to be 1099 pairs/s. We have to emphasize that the

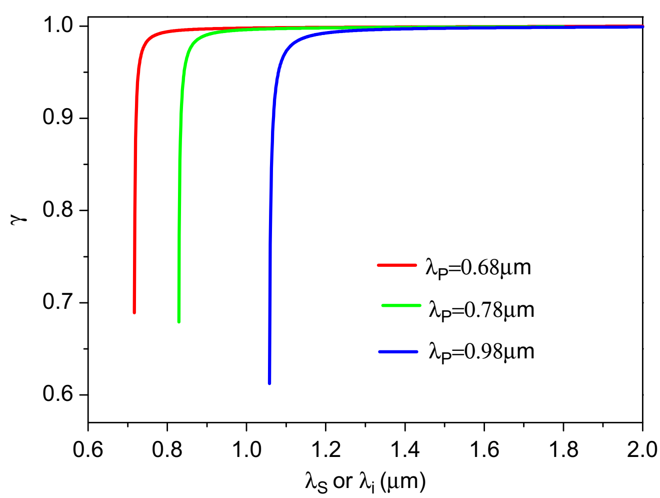

Fig. 2. Variation of parameter γ as a function of the wavelength of signal or idler photon. The wavelengths of pump photon are 680 nm, 780 nm and 980 nm. The working temperature is 160 °C.

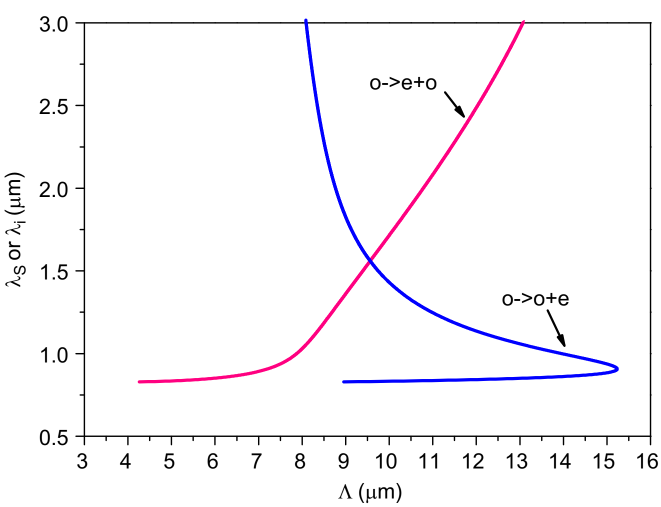

Fig. 3. Two SPDC processes of ordinary pump photon to either extraordinary signal and ordinary idler paired photons or conversely simultaneously. The wavelength of signal photon or idler photon is a function of the grating period. The wavelength of pump photon is 780 nm and the working temperature is 160 °C.

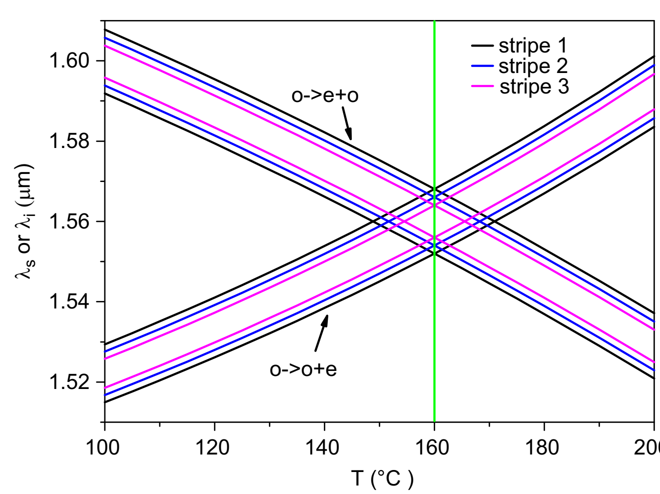

Fig. 4. For three-stripe DPPLN, the wavelength of signal photon or idler photon varies with the working temperature. The wavelength of pump photon is 780 nm. The desired hyperentangled state emerges at 160 °C.

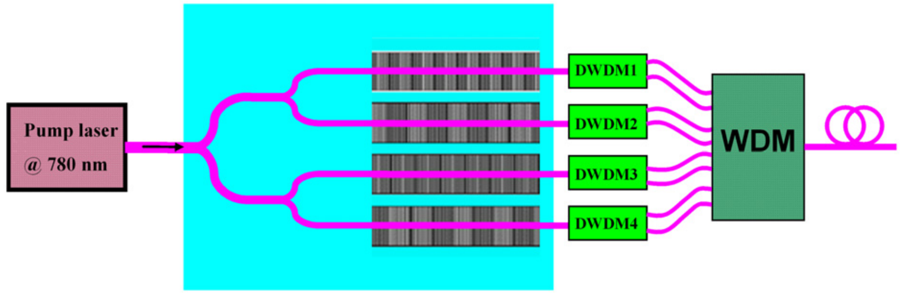

Fig. 5. Schematic description of four-dimensional frequency and cross-polarized hyperentanglement photon-pair generation by type-II SPDC in a four-stripe Ti-indiffused DPPLN waveguide.

number of polarization-frequency hyperentangled photon pairs is less than 1099 pairs/s since we should collect the photon pairs from each stripe into the same spatial mode. The spatial indistinguishability can be achieved by the single mode fiber coupling or by far field collection.

Here we propose another feasible experimental scheme by using the lithium niobate waveguide [24,31] besides the bulk crystal. Since when propagating in optical waveguide, light can be easily confined and maintain their energy. This will improve the efficiency of the entangled photon generation. Fig. 5 is the schematic description of four-dimensional frequency and cross-polarized hyperentangled photon-pair generation from titanium indiffused lithium niobate waveguide. After being collected into the same spatial mode such as polarization maintaining fiber, the source serves as a compact and bright hyperentangled photon source. By using demultiplexer for wavelength division multiplex (DWDM), we can separate a pair of specific wavelengths generated by SPDC before they enter different input ports of WDM device. We can use WDM filters to combine several of these together to form a superposition of carrier wavelengths. After a long distance of propagation, by using a demultiplexer, different frequencies will emit from different ports. Each two customers in quantum network will share a frequency pair from two ports and use the cross-polarized entanglement for quantum information processing, etc. N frequency pairs then can serve for N pairs of customers. Integrated quantum photonics [32–34] based on optical waveguide opens the way for miniaturization, scalability, complexity and improving the performance of photonic quantum circuits for future quantum technologies.

For the four-dimensional frequency and nondegenerate cross-polarization hyperentangled state generation, we design a four-stripe titanium indiffused DPPLN waveguide which covers the wavelengths of 1552 nm/1568 nm, 1554 nm/1566 nm, 1556 nm/1564 nm, and 1558 nm/1562 nm when the pump is 780 nm. The working temperature is designed to be 160 °C. We set $P = 1.0$ mW, $L = 20$ mm, $d_{24} = 4.6$ pm/V. Suppose that the section of titanium indiffused waveguide is 9 μm × 9 μm. We should consider the overlap integrals between the pump, signal, and idler over the transverse coordinates [24]. The effective interaction area is then defined as the ratio between the product of pump, signal and idler mode areas and the square of overlap integral [35]. The values of Δn_o and Δn_e at the pump, signal, and idler wavelengths are considered following Refs. [24,36]. By substituting this effective area into the formula of photon-pairs generation rate, we can get the generation rate of photon pairs roughly equals to 1.74084×10^7 pairs/s. But in fact the photon-pair number collected into the single mode fiber is less than this theoretical value due to the coupling loss.

In this work, both the bulk and waveguide multi-stripe DPPLN are discussed, which are different from techniques using the natural broadband frequency correlation in SPDC [37,38], we using multi-stripe DPPLN to generate high-dimensional frequency-entanglement. Compared with the doubly periodic gratings are placed in series in the substrate, our device has the advantage in the same propagation crystal length (small temporal walk-off) and controllable propagation phase for each pair after the crystal. For multi-stripe DPPLN, the initial phase for each pair is the same and the propagation phase of each pair after the crystal can be controlled separately, while for the DPPLNs placed in series, the initial phase for each frequency pair is different and after the crystal the phase cannot but has to be controlled separately since each pair will propagate through different crystal length. On the other hand, for a short duration pump pulse, considering the group velocity dispersion, the parallel DPPLNs are preferred for smaller temporal walk-off.

It is worth to mention that for the generation and collection of such hyperentangled photon pairs one may pay more efforts in the phase stabilization. The multi-stripe DPPLN waveguide should be temperature controlled and no phase difference between each stripe should be introduced into the pump before it splits into photon pair. Also before collecting the photon pairs into the single mode fiber or under a far field condition, the difference of phase accumulation between each frequency pair should be stabilized as $2\pi * n$ ($n = 1,2,3,\ldots$). The frequency bins have to be summed up after all the stripes in a coherent manner at the output of the Mach–Zehnder (MZ) interferometer. The relative phase between all the components will drift anyway, and maintaining a coherent superposition of all the frequency-bin contributions implies tolerating phase drifts no larger than $2\pi/100$ or so before degrading the entanglement quality. This would probably necessitate an active stabilization of the MZ interferometer by using a reference laser, to measure the phase in real time and feedback a piezo stretcher, and that laser might be itself stabilized against an atomic transition. It might also be necessary to frequency stabilize the pump laser itself to maintain its overall phase over a long term.

Although great efforts should be paid, it is feasible to prepare such a frequency-polarization hyperentangled state. But to distribute such hyperentangled photon pairs over long distance through optical fibers is of great challenge [38,39]. Even though, such a bright hyperentangled state may be utilized for entanglement degree of freedom (DOF) transfer locally. Since polarization entanglement DOF can transfer onto other photonic DOFs, as reported in [40]. We may achieve discrete frequency-entanglement DOF transferred from the polarization entanglement DOF, then we can create and control discrete frequency state by using a hybrid quantum gate. There are two technologies to analysis frequency-bin entanglement. One is the technology of electro-optical modulators (EOMs), as reported in [37,38]. The other is the technology of nonclassical interference to quantify the amount of entanglement such as by reconstructing a restricted density matrix [40], and by Hong–Ou–Mandel type interferometer

[41,42]. Our frequency-bin entanglement cannot use the current technology of electro-optical modulators for the analysis settings.

4. Conclusion

In summary, we have proposed a scheme for the generation of both nondegenerate cross-polarization-entangled and high-dimensional frequency-entangled photon pair using a multi-stripe DPPLN crystal. Hyperentangled photon pairs produced from optical waveguide are extremely compact, better efficiency, and stable. Combined with simultaneous entanglement in other degrees of freedom, this type of photon source will certainly prompt the developments of quantum communication science with better security and higher capacity. This type of hyperentangled state may work as an initial state for the local transferring between different DOF entanglements. Another advantage of this hyperentangled photon source lies in the flexible quasi-phase-matching technique, enabling a feasible engineering on the frequency degree. We can obtain frequency-entangled photon pairs at the telecom S-band (1490−1528 nm), C-band (1528−1568 nm) and L-band (1568−1610 nm) for long-distance quantum communication. We can also obtain different types of frequency-entangled photon pairs such as the telecom wavelength for quantum communication and the atomic absorbing for quantum storage.

Acknowledgments

This work was supported by the State Key Program for Basic Research in China (Nos. 2011CBA00205, 2012CB921802), the National Natural Science Foundations of China (Nos. 10904066, 11021403, 91121001), the Project Funded by the Priority Academic Program Development of Jiangsu Higher Education Institutions (PAPD), and a Foundation for the Author of National Excellent Doctoral Dissertation of PR China (FANEDD).

References

[1] C.H. Bennett, S.J. Wiesner, Physics Review Letters 69 (1992) 2881.
[2] C.H. Bennett, Physics Review Letters 68 (1992) 3121.
[3] C.H. Bennett, G. Brassard, et al., Physics Review Letters 70 (1993) 1895.
[4] P.G. Kwiat, Journal of Modern Optics 44 (1997) 2173.
[5] J.T. Baeeriro, T.C. Wei, P.G. Kwiat, Nature Physics 4 (2008) 282.
[6] C. Wang, L. Xiao, W.Y. Wang, G.Y. Zhang, G.L. Long, Journal of the Optical Society of America B 26 (2009) 2072.
[7] S.P. Walborn, S. Pádua, C.H. Monken, Physical Review A 68 (2003) 042313.
[8] C. Schuck, G. Huber, C. Kurtsiefer, H. Weinfurter, Physics Review Letters 96 (2006) 190501.
[9] T.C. Wei, J.T. Barreiro, P.G. Kwiat, Physical Review A 75 (2007) 060305.
[10] J.T. Barreiro, N.K. Langford, N.A. Peters, P.G. Kwiat, Physics Review Letters 95 (2005) 260501.
[11] W.B. Gao, C.Y. Lu, et al., Nature Physics 6 (2010) 331.
[12] A. Chiuri, G. Vallone, et al., Physics Review Letters 105 (2010) 250501.
[13] S. Tanzilli, H.D. Riedmatten, et al., Electronics Letters 37 (2001) 26.
[14] X.Q. Yu, P. Xu, et al., Physics Review Letters 101 (2008) 233602.
[15] H.Y. Leng, X.Q. Yu, et al., Nature Communications (2011) 1439, http://dx.doi.org/10.1038/ncomms.
[16] S.E. Harris, Physics Review Letters 98 (2007) 063602.
[17] M.B. Nasr, S. Carrasco, et al., Physics Review Letters 100 (2008) 183601.
[18] H.C. Lim, A. Yoshizawa, H. Tsuchida, K. Kikuchi, Optics Express 16 (2008) 16052.
[19] P.G. Kwiat, K. Mattle, et al., Physics Review Letters 75 (1995) 4337.
[20] P.G. Kwiat, E. Waks, A.G. White, I. Appelbaum, P.H. Eberhard, Physical Review A 60 (1999) R773.
[21] M. Fiorentino, G. Messin, C.E. Kuklewicz, F.N.C. Wong, J.H. Shapiro, Physical Review A 69 (2004) 041801.
[22] S.M. Gao, C.X. Yang, Optics Letters 32 (2007) 2653.
[23] S.M. Gao, C.X. Yang, Journal of the Optical Society of America B 25 (2008) 734.
[24] K. Thyagarajan, J. Lugani, et al., Physical Review A 80 (2009) 052321.
[25] M.H. Chou, K.R. Parameswaran, M.M. Fejer, I. Brener, Optics Letters 24 (1999) 1157.
[26] Z.W. Liu, Y. Du, et al., Journal of the Optical Society of America B 19 (2002) 1676.
[27] Y.X. Gong, Z.D. Xie, et al., Physical Review A 84 (2011) 053825.
[28] M.H. Rubin, D.N. Klyshko, Y.H. Shih, V. Sergienko, Physical Review A 50 (1994) 5122.
[29] M.H. Rubin, Physical Review A 54 (1996) 5349.
[30] J. Svozilik, J. Perina, Physical Review A 80 (2009) 023819.
[31] J. Lugani, S. Ghosh, K. Thyagarajan, Physical Review A 83 (2011) 062333.
[32] S.V. Zhukovsky, D. Kang, et al., Optics Letters 36 (2011) 3548.
[33] A. Politi, J.C.F. Matthews, M.G. Thompson, J.L. O' Brien, IEEE Journal of Selected Topics in Quantum Electronics 15 (2009) 1673.
[34] S. Tanzilli, A. Martin, et al., Laser Photonics Review (2011) 1.
[35] G.D. Xu, Y.H. Wang, Y.Y. Zhu, S.N. Zhu, N.B. Ming, Journal of the Optical Society of America B 21 (2004) 568.
[36] S. Fouchet, A. Carenco, C. Daguet, R. Guglielmi, L. Riviere, Journal of Lightwave Technology 5 (1987) 700.
[37] L. Olislager, J. Cussey, et al., Physical Review A 82 (2010) 013804.
[38] L. Olislager, I. Mbodji, et al., arxiv:1107.5519v1, 2011.
[39] M. Shtaif, C. Antonelli, M. Brodsky, arxiv:1012.2013v1, 2010.
[40] S. Ramelow, L. Ratschbacher, A. Fedrizzi, N.K. Langford, A. Zeilinger, Physics Review Letters 103 (2009) 253601.
[41] Y.J. Lu, R.L. Campbell, Z.Y. Ou, Physics Review Letters 91 (2003) 163602.
[42] Y.F. Bai, P. Xu, Z.D. Xie, Y.X. Gong, S.N. Zhu, Physical Review A 85 (2012) 053807.
[43] I. Shoji, T. Kondo, A. Kitamoto, M. Shirane, R. Ito, Journal of the Optical Society of America B 14 (1997) 2268.